Barrier-Bound Resonances in Semiconductor Superlattices in Strong Magnetic Fields

T. Duffield, R. Bhat, M. Koza, F. DeRosa, K. M. Rush, and S. J. Allen, Jr.
Bell Communications Research, Inc., Redbank, New Jersey 07701
(Received 13 May 1987)

The effective "miniband" mass approximation is shown to break down in strong magnetic fields when the magnetic length is smaller than the superlattice period. Under these conditions a real-space description must be used and features in the inhomogeneously broadened cyclotron resonance can be indexed by the position of the cyclotron orbit with respect to the barriers and wells. The line shape agrees with a calculation of the quantum states in a magnetic field in a one-dimensional periodic potential and these experiments give us a rare view of Landau states in the limit where the periodic potential has a period that is larger than the cyclotron diameter.

PACS numbers: 73.20.Dx, 71.25.Jd, 72.20.My

The effective-mass approximation is the cornerstone of our understanding of electron transport in solids in periodic potentials. The validity of the effective-mass approach requires that the characteristic length of the probe be much larger than the wavelength of the periodic potential. In the case of cyclotron resonance, which is the most powerful technique for the measure of the effective mass in solids, this requires that the cyclotron diameter be large compared with the period of the potential. Although most normal solids invariably satisfy this condition, the character of electron states in a magnetic field when this condition is not satisfied was first discussed by Harper[1,2] as early as 1955. In the intervening years this problem has attracted repeated theoretical discussion,[3-5] but only with the invention and perfection of semiconductor superlattices do we have the opportunity of addressing these issues experimentally. Here we fabricate semiconductor superlattices with periodic potentials that can assume arbitrary scale with respect to the cyclotron diameter and show how cyclotron resonance appears when the effective "miniband" mass approximation breaks down.

In previous work Mann and co-workers[6-8] discussed theoretically the problem of electrons moving in a one-dimensional periodic potential in a semiconductor superlattice and showed experimentally[6,7] that well defined Landau levels can be seen in interband magnetoluminescence only for transitions that originate within the combined electron and hole minibands. Here we directly perform cyclotron resonance (CR) in the limit that the period is larger than the magnetic length. In this limit the CR appears inhomogeneously broadened with features that can be qualitatively understood in terms of classical orbits whose character is dictated by the orbit position with respect to the superlattice barriers and wells. A quantum mechanical calculation is performed and agreement is achieved with the experimental results.

The superlattices, 6 μm thick, were grown by organometallic chemical vapor deposition on semi-insulating GaAs. The barriers, comprised of $Al_xGa_{1-x}As$ with $x \simeq 0.3$, were nominally 2 nm thick. To minimize impurity scattering and to keep the plasma frequency well below the cyclotron-resonance frequency, the superlattice was lightly doped to levels of $n \gtrsim 10^{15}$ cm^{-3} (see Duffield *et al.*[9]). Cyclotron resonance was observed by our measuring the absorption of far-infrared radiation when a magnetic field was applied in the plane of the sample—the Voigt geometry (see Fig. 1). The electric vector of the radiation field was polarized perpendicular to the magnetic field. To avoid carrier freezeout, experiments were performed at temperatures above 60 K.

At the largest magnetic field at our disposal, 8 T, the cyclotron diameter was of the order of 20 nm. The periods of the superlattices that we have investigated are 10, 20, 30, 50, and 60 nm. The results for the 10-nm-period superlattice have been discussed elsewhere and can be described by cyclotron resonance in the effective-mass approximation.[9] The results for the larger periods all showed qualitatively different behavior from this classical result. We describe in some detail experiment and theory for the 20- and 50-nm-period samples. The re-

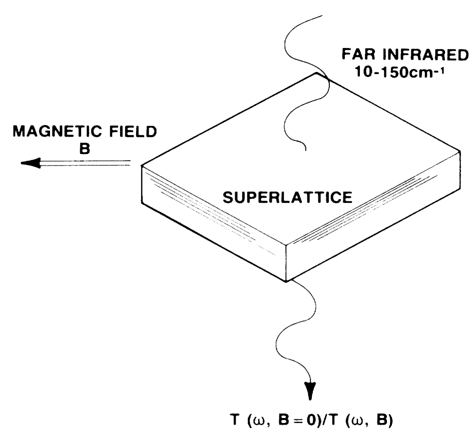

FIG. 1. Sample orientation with respect to applied magnetic field. Resonance determined from ratio of transmission in zero field, $T(\omega,B=0)$, to transmission in a field, $T(\omega,B)$.

sults embrace the essential features of cyclotron resonance when the magnetic length is less than the superlattice period.

Figure 2(a) shows the absorption for a magnetic field of 7.18 T applied to a 50-nm-period superlattice. Qualitatively the resonance may be characterized as an extremely inhomogeneously broadened line. The source of the inhomogeneity can be appreciated by reference to Fig. 3(a). When the cyclotron diameter is smaller than the superlattice period the resonance condition critically depends on the position of the orbit with respect to the barriers and wells. The classical orbits, depicted in Fig. 3(a), correspond to (1) tunneling resonances for orbits impaled on the barrier, which lie below the bulk CR, since the electron must tunnel twice per cycle; (2) well-bound resonances that are shifted above the bulk CR since they experience an additional restoring force due to confinement between the barriers; and (3) skipping orbits that resonate at frequencies close to the harmonics of bulk CR. The latter two features are also present in Voigt-geometry cyclotron-resonance experiments in space-charge layers,[10] whereas the tunneling resonance is peculiar to superlattice systems.

Belle, Mann, and Weimann[6] showed that the electron states in a 1D potential in a magnetic field can be determined by diagonalization of the following Hamiltonian:

$$H=-\frac{\hbar^2}{2m}\frac{\partial^2}{\partial z^2}+\tfrac{1}{2}m\omega_c^2z^2+V(z+z_0), \qquad (1)$$

where $\hbar$ and m are Planck's constant and the electron mass in GaAs, ω_c is the cyclotron frequency in GaAs, $V(z)$ is the periodic potential, and z_0 is the position of the orbit center. The results of this calculation for a period of 50 nm are shown in Fig. 3(b). In the bulk material these Landau levels are straight lines, with energy independent of the orbit center, indicated in the figure by

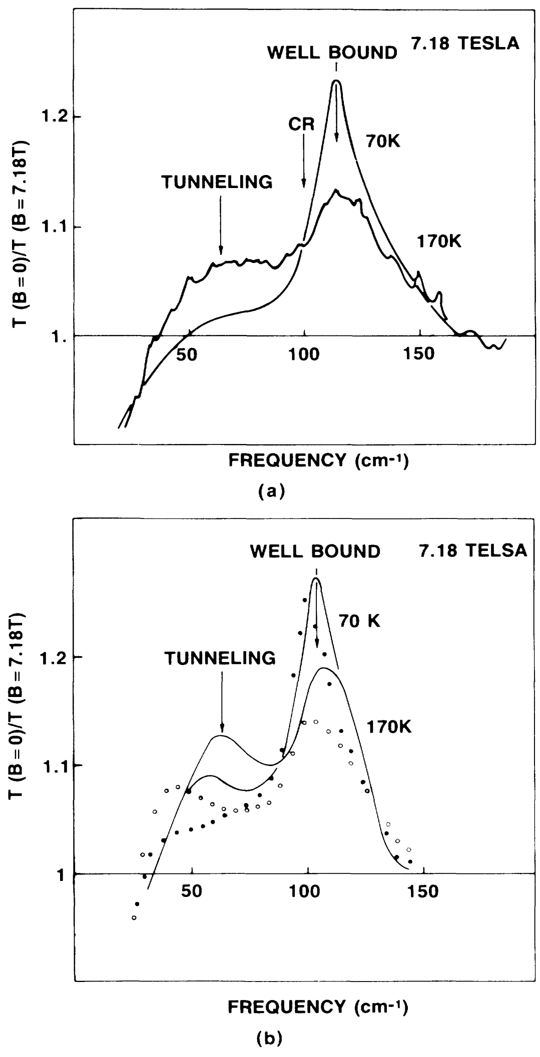

FIG. 2. (a) Cyclotron resonance in the 50-nm-period superlattice at temperatures of 70 and 170 K. CR indicates the position of bulk GaAs cyclotron resonance. (b) Calculated absorption spectrum for a 50-nm-period superlattice with barriers 0.1 eV high by 2 nm wide at 70 and 170 K, solid lines, and with barriers 0.2 eV by 2 nm wide at 70 and 170 K, filled and open circles, respectively.

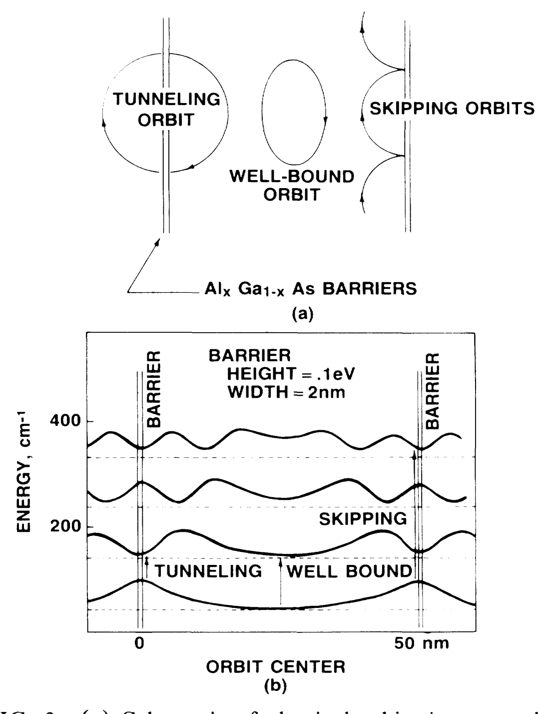

FIG. 3. (a) Schematic of classical orbits in a superlattice when the orbit diameter is less than the period. (b) Landau-level energies in a field of 7.18 T vs orbit position for 50-nm-period superlattice. Arrows indicate the quantum-mechanical transitions that have the classical analogs indicated in (a). Dashed lines indicate Landau levels in the absence of the barriers.

dashed lines. The transitions indicated by the arrows are the quantum-mechanical analogs of the classical orbits shown in Fig. 3(a).

From these states we can express the frequency-dependent mobility tensor for an electron at z_0 as follows:

$$\mu_{nm}^{zz} = i\omega_{nm}(e\,|\langle n|z|m\rangle|^2/\hbar)\{[\omega+\omega_{nm}(z_0)]^{-1}+[\omega-\omega_{nm}(z_0)]^{-1}\},\quad \mu_{nm}^{yy}=\mu_{nm}^{zz}\omega_c^2/\omega_{nm}^2,$$
$$\mu_{nm}^{yz} = \omega_c(e\,|\langle n|z|m\rangle|^2/\hbar)\{[\omega+\omega_{nm}(z_0)]^{-1}-[\omega-\omega_{nm}(z_0)]^{-1}\}. \tag{2}$$

Here ω_{nm} is the transition frequency from level n to level m at position z_0, e is the electron charge, and ω is the applied frequency. Below we introduce a relaxation time broadening by substituting $\omega+i/\tau$ for ω.

The frequency-dependent conductivity tensor may be expressed as

$$\sigma^{\alpha\beta} = \sum_n \sum_{m>n} \int_{-p/2}^{p/2} \frac{dz_0}{p} e\mu_{nm}^{\alpha\beta} G\{\exp[-\hbar\omega_n(z_0)/kT]-\exp[-\hbar\omega_m(z_0)/kT]\}, \tag{3}$$

where

$$G = N\left[\sum_n \int_{-p/2}^{p/2} \frac{dz_0}{p}\exp[-\hbar\omega_n(z_0)/kT]\right]^{-1}. \tag{4}$$

Here $\hbar\omega_n$ is the energy of the nth Landau level at z_0. N is the electron density in the superlattice and p the superlattice period. We then calculate the submillimeter wave absorption using (3) and Maxwell's equations in the Voigt geometry.

The calculated absorption for the 50-nm-period superlattice with barriers 0.1 eV high by 2 nm wide and 0.2 eV by 2 nm wide is shown in Fig. 2(b), for two different temperatures. The model gives best account of the experimental data for a barrier strength of 0.1 eV by 2 nm. *The extremes of the line shape reflect the extremes of the joint density of states and may be ascribed to tunneling resonances centered on the barrier and well-bound resonances centered on the center of the well.*

The temperature dependence can be understood as follows. The lowest Landau levels are repelled by the barriers. As a result, transitions due to orbits impaled on the barriers will not be favored at low temperatures. At elevated temperatures some electrons will thermally populate these orbits and a low-frequency shoulder develops at the expense of the strong well-bound resonance. Since the tunneling resonance is a cyclotron resonance which requires the electron to tunnel through the barrier twice per cycle, it should be a direct measure of the tunneling rate.

To test our understanding we have also calculated the response for the 20-nm-period superlattice and compared with experiment. Figure 4 shows the Landau levels for this case. Here we see that the well-bound resonance is pushed to much higher frequency and we expect the low-frequency absorption to be dominated by the tunneling resonances indicated by the arrows in the figure.

The results of the model calculation for two different barrier strengths and of the experiment are compared in Fig. 5. The overall agreement is satisfactory for a barrier strength of 0.1 eV by 2 nm, as we had found for the

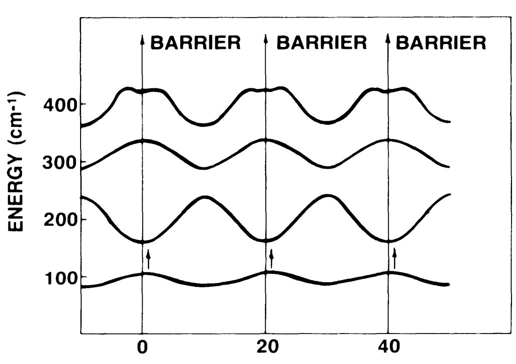

FIG. 4. Landau-level energies vs orbit position for 20-nm-period superlattice. Barriers are 0.1 eV by 2 nm. $B=7.5$ T. The tunneling resonances are indicated by the arrows.

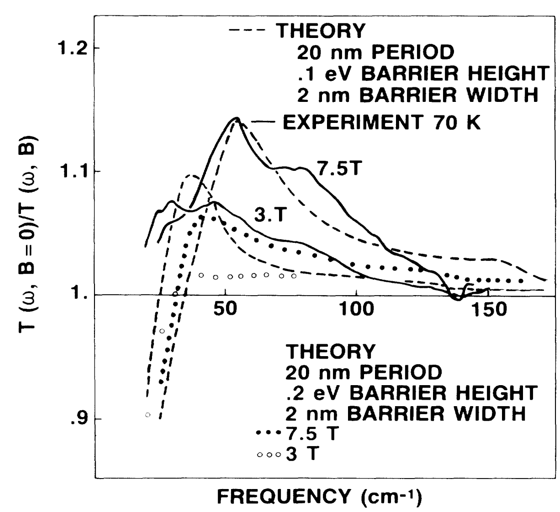

FIG. 5. Solid lines, experimental absorption for two different magnetic fields in a superlattice with a period of 20 nm. Dashed lines, calculated absorption for a barrier strength of 0.1 eV by 2 nm. Open circles and filled circles, calculated absorption for a barrier strength of 0.2 eV by 2 nm.

50-nm-period superlattice. There are reproducible features that are not predicted by the model calculation and we can offer no explanation for them here. We do not feel that they comprise the overall success of the model. The general agreement indicates that the low-frequency absorption can be ascribed to barrier-bound resonances in which the electron tunnels twice per cycle through a superlattice barrier. The extreme low-frequency peak is due to an orbit centered on the barrier. The well-bound resonance appears in this limit as a weak shoulder at 160 cm^{-1} and is not seen experimentally.

We have fitted these data with a bulk GaAs mass of 0.07 and dielectric function of 13 and adjusted the product of height by width of the barrier. It should be noted that best agreement is achieved with a product roughly half of the nominal values, 0.2 eV by 2 nm, that were targeted during growth. In consideration that these materials were grown by organometallic chemical vapor deposition the barrier width is more uncertain than the height. The real-space calculations that we have performed do describe the data at short periods, 10 nm, with material parameters that closely approximate the targeted and measured growth parameters and which can alternatively be described by cyclotron resonance in a miniband.[9] At present we have not been able to measure the product of barrier height by width for the large-period superlattices with sufficient accuracy to resolve this issue. We do not think that this issue compromises our identification and description of the cyclotron resonance in this limit.

In summary, we have observed the spectrum of electronic transitions that occur in periodic potentials when subjected to magnetic fields sufficiently intense that the magnetic length is less than the potential period. We have modeled these excitations and given a quantitative description of the observed spectra. Most interesting are the features related to tunneling through individual barriers which are sensitive and specific to material structure and composition. Skipping orbits have yet to be seen in these materials and will require a more systematic exploration of parameter space. In a more lengthy publication we will explore in more detail the temperature and magnetic field dependence as well as the relationship of the material parameters to the fit parameters.

[1]P. G. Harper, Proc. Phys. Soc. London, Sect. A **68**, 879 (1955).

[2]P. G. Harper, J. Phys. Chem. Solids **82**, 495 (1967).

[3]R. Rammal, J. Phys. (Paris) **46**, 1345 (1985).

[4]P. L. Taylor, Phys. Rev. B **15**, 3558 (1977).

[5]D. R. Hofstadter, Phys. Rev. B **14**, 2239 (1976), and references contained therein.

[6]G. Belle, J. C. Mann, and G. Weimann, Surf. Sci. **170**, 611 (1986).

[7]G. Belle, J. C. Mann, and G. Weimann, Solid State Commun. **56**, 65 (1985).

[8]J. C. Mann, in *Two-Dimensional Systems, Heterostructures, and Superlattices,* edited by G. Bauer *et al.*, Springer Series on Solid State Sciences Vol. 53 (Springer-Verlag, New York, 1984), p. 183, and to be published.

[9]T. Duffield, R. Bhat, M. Koza, F. DeRosa, and D. M. Hwang, P. Grabbe, and S. J. Allen, Jr., Phys. Rev. Lett. **56**, 2724 (1986).

[10]W. Zhao, C. Mazure, F. Koch, J. Ziegler, and H. Maier, Surf. Sci. **142**, 400 (1984), and references contained therein.